2014

Enantiomeric Selective Adsorption of Amino Acid by Polysaccharide Composite Materials

Simon Duri
Marquette University, simon.duri@marquette.edu

Chieu D. Tran
Marquette University, chieu.tran@marquette.edu

Enantiomeric Selective Adsorption of Amino Acid by Polysaccharide Composite Materials

Simon Duri
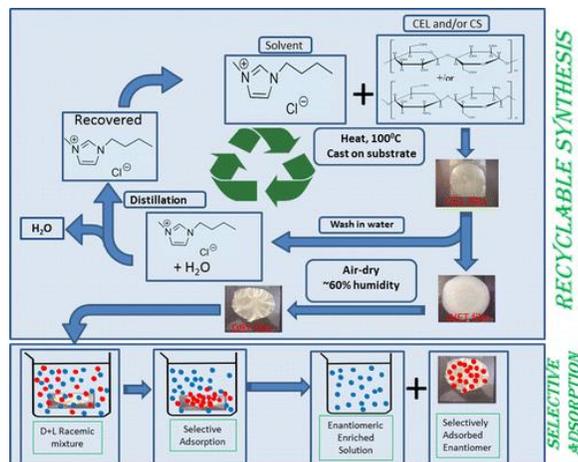Department of Chemistry, Marquette University, Milwaukee, Wisconsin
Chieu D. Tran
Department of Chemistry, Marquette University, Milwaukee, Wisconsin

SUBJECTS:

High-performance liquid chromatography, Composites, Adsorption,

Abstract

A composite containing cellulose (CEL) and chitosan (CS) synthesized by a simple and recyclable method by using butylmethylimmidazolium chloride, an ionic liquid, was found to exhibit remarkable enantiomeric selectivity toward the adsorption of amino acids. The highest adsorption capacity and enantiomeric selectivity are exhibited by 100% CS. A racemic amino acid can be enantiomerically resolved by 100% CS in about 96–120 h. Interestingly, adsorption by 50:50 CEL/CS is more similar to that by 100% CS than to 100% CEL. Specifically, whereas 100% CEL has the lowest adsorption capacity and enantiomeric selectivity, 50:50 CEL/CS has sufficient enantiomeric selectivity to enable it to be used for chiral resolution. This is significant because in spite of its high enantiomeric selectivity 100% CS cannot practically be used because it has relatively poor mechanical properties and undergoes extensive swelling. Adding 50% CEL to CS substantially improves the mechanical properties and reduces its swelling while it retains sufficient enantiomeric selectivity to enable it to be used for routine chiral separations. The kinetic results indicate that the enantiomerically selective adsorption is due not to the initial surface adsorption but rather to the subsequent stage in which the adsorbate molecules diffuse into the pores within the particles of the composites and consequently are adsorbed by the interior of each particle. The strong intermolecular and intramolecular hydrogen bond network in CEL enables it to adopt a very dense structure that makes it difficult for adsorbate molecules to diffuse into its interior, thereby leading to low enantiomeric selectivity. Compared to hydroxy groups, amino groups cannot form strong hydrogen bonds. The hydrogen bond network in CS is not as extensive as in CEL, and its inner structure is relatively less dense than that of CEL. Adsorbate molecules can, therefore, diffuse from the outer surface to its inner structure relatively more easily than in CEL, thereby leading to higher enantiomeric selectivity for 100% CS.

Introduction

Differences between the physiological properties and the therapeutic effects of the enantiomeric forms of many compounds have been recognized for some time.(1-4) Very often, only one form of an enantiomeric pair is pharmacologically active. The other or others can reverse or otherwise limit the effect of the desired enantiomer. However, despite this knowledge, only 61 of 528 chiral synthetic drugs are marketed as single enantiomers whereas the other 467 are sold as racemates.(1) Recognizing the importance of chiral effects, the FDA in 1992 issued a mandate requiring pharmaceutical companies to evaluate the effects of individual enantiomers and to verify the enantiomeric purity of chiral drugs that are produced.(1-4) It is thus hardly surprising that the pharmaceutical industry needs effective methods for the optical resolution of racemic mixtures on the preparative scale. Conventional chiral resolution methods, including preferential crystallization, stereoselective transformation by an optical resolution agent, high-performance liquid chromatography and electrophoresis have common shortcomings such as relatively low productivity, expensive chemical

consumables, and high energy consumption.(5-10) The use of membrane technology for chiral separations offers several advantages over traditional methods, including low time cost, simplicity of operation, and easy scale-up.(5-10) Furthermore, when using chiral activated membranes only a small quantity of an expensive chiral selector is required.(8-10)

Polysaccharides are chiral polymers that can potentially be used as chiral membranes for enantiomeric separations. Chitosan (CS) and cellulose (CEL) are two of the most widely used polysaccharides. Chitosan (CS) is a linear amino polysaccharide obtained by N-deacetylation of chitin, and chitin is the second most abundant naturally occurring polysaccharide after cellulose (CEL).(11-14) CS's structure allows it to have some unique properties, including antimicrobial, drug delivery, wound healing, hemostasis, and pollutant adsorbant.(12-28) In addition, CS is also biocompatible and biodegradable. Unfortunately, in spite of its potential, there are drawbacks that severely limit the application of CS. For example, similar to cellulose (CEL), the most abundant substance on earth, in CS a network of intrahydrogen and interhydrogen bonds enables it to adopt an ordered structure.(15-22) Although such a structure is responsible for CS having the aforementioned properties and CEL having superior mechanical strength, it also makes them insoluble in most solvents.(15-22) As a consequence, high temperature, strong exotic solvents, and strong acid followed by neutralization with base are needed to dissolve CEL and CS, respectively. These methods are undesirable because they are based on the use of corrosive and volatile solvents, require high temperature, and suffer from side reactions and impurities that may lead to changes in the structure and properties of the polysaccharides. More importantly, it is not possible to use a single solvent or system of solvents to dissolve both CEL and CS. Furthermore, CS is known to swell in water, which leads to structural weakening in wet environments.(15-22) To increase the structural strength of CS products, attempts have been made to covalently bind or graft CS onto man-made polymers to strengthen its structure.(15-25) Such modification is not desirable because it may inadvertently alter the CS properties, making it nonbiocompatible and toxic and lessening or removing its unique properties. A new method that can effectively dissolve both CS and CEL not at high temperature and not by corrosive and volatile solvents but rather by recyclable "green" solvents is particularly needed.

We have demonstrated recently that a simple ionic liquid, $BMIm^+Cl^-$, can dissolve both CEL and CS, and by the use of $BMIm^+Cl^-$ as the sole solvent, we developed a simple, green, and totally recyclable method to synthesize [CEL+CS] composites just by dissolution without using any chemical modifications or reactions.(23-25) The [CEL+CS] composite obtained was found not only to be biodegradable and biocompatible but also to retain the unique properties of its components, namely, superior mechanical strength (from CEL) and excellent antibacterial and adsorption capability for pollutants and toxins (from CS).(23-25)

Because the [CEL+CS] composite was synthesized without employing any chemical modifications, the chiral nature of its components remains intact, and it is possible that it may be used as a chiral membrane for the enantiomeric separation of racemic mixtures. Such considerations prompted us to initiate this study, which aims to hasten the breakthrough by using the [CEL+CS] composite synthesized by the green, recyclable method that we have developed recently, for chiral separation. Results for enantiomeric differentiation with respect to the adsorption of different amino acids by the [CEL+CS] composite and the mechanism of the chiral adsorption deduced from adsorption kinetics of composites having different concentration of CEL and CS will be reported herein.

Experimental Section

The polysaccharide composite materials used in this study were prepared according to procedures previously developed in our laboratory.(23-25)d and l enantiomers (99%) of tryptophan (Trp), tyrosine (Tyr), histidine (His), and phenylalanine (Phe) were obtained from Alfa Aesar. Experiments with racemic mixtures were carried out on a Shimadzu LC-20AT prominence liquid chromatograph equipped with an SPD-20A prominence UV/vis detector.

The chiral column used was a 250 L × 4.6 mm i.d. 5-µm-particle stainless steel column (Advance Separation Technologies, Whippany, NJ, Chirobiotic TAG column). The mobile phase for Trp, Tyr, and Phe was 60:40 methanol/water, and His was separated using 30:70 ethanol/water in 160 mM sodium phosphate buffer adjusted to pH 4.5; the flow rate was 1.0 mL/min. Trp and Tyr were detected at 275 nm, and His and Phe were detected at 205 nm. Experiments with optically active (pure enantiomer) samples were carried out on a PerkinElmer Lambda 35 UV/visible spectrometer.

For the enantiomeric resolution experiments, about 0.3 g of the dry polysaccharide composite material was placed in a sample vial. The dl racemic solution of the amino acid (30 mL, 1.0×10^{-3} M) was added. (The concentration of both the d and the l enantiomers in this solution was 5.0×10^{-4} M.) The amino acid solutions were prepared in distilled deionized water at pH 6.6. The vials were tightly closed and agitated (at room temperature) at 240 osc/min on a mechanical shaker (model E6005 explosion proof reciprocal shaker, Eberbach Corporation, Ann Arbor, MI). At specific time intervals, 20 µL solutions were withdrawn and injected into the HPLC for analysis. It is possible that for racemic mixtures the presence of one enantiomer may have some effect on the adsorption of other enantiomers. To determine if such an effect is present, the adsorption of optically active (pure) d and l enantiomers was measured separately by UV/vis spectrophometry. The experimental setup and conditions (mass of film and volume of solution) were the same as those used for the racemic mixture. The concentration of the optically active solutions used for this experiment was 5.0×10^{-4} M. This concentration is the same as that of the individual enantiomers used for the racemic experiment described above. In addition, because these were solutions of pure enantiomers, the residual concentration of the enantiomer in solution at specific time intervals was directly determined by UV/vis absorption. After the UV absorption of the solution was measured, the sample solution was returned to its sample vial to ensure that there were no significant volume changes in the sample during the course of the experiment.

Results and Discussion

HPLC chiral separation was carried out to determine the adsorption of d- and l-Tyr enantiomers from a solution of a 1.0×10^{-3} M racemic mixture using three different polysaccharide composite materials: 100% CS, [CEL+CS], and 100% CEL. The obtained chromatograms are shown in Figure 1. As expected, the HPLC chromatograms contain two bands corresponding to the two enantiomers in solution (d and l). The identity of each band was determined by spiking the racemic solutions with one of the enantiomers and identifying the band whose intensity increased as a result of the enantiomer in the spike. In all cases, the l enantiomer was eluted first (this band is indicated by an arrow in Figure 1). The second unlabeled band corresponds to the d enantiomer. The intensity of the two bands was found to decrease with time. However, as indicated by the arrow in the figure, the intensity of the l enantiomer decreases relatively faster than that of the d enantiomer. For the 100% CS composite, the band for the l enantiomer decreases and disappears completely after about 96 h whereas the band for the d enantiomer had changed only slightly. For the [CEL+CS] composite, about 288 h was required for the band of the l enantiomer to disappear. For the 100% CEL composite, both bands were still present in the chromatograms even after 288 h. However, even though both bands were still present, the intensity of the l enantiomer band decreased more than that of the d enantiomer. Similar results were also found for Trp, His, and Phe. The results seem to suggest that these polysaccharide composite materials selectvively adsorb more of the l enantiomer than the d enantiomer. Such selective adsorption of one enantiomer over the other can lead to an enrichment of the racemic mixtures that potentially could be used for enantiomeric resolution. Results also indicate that the rate at which the intensity of the l band decreases seems to be dependent on the polysaccharide composite used. For example, it took about 96 h for the l band to disappear with the 100% CS composite whereas the [CEL+CS] composite required about 288 h. For the 100% CEL, both HPLC bands were still present even after 288 h.
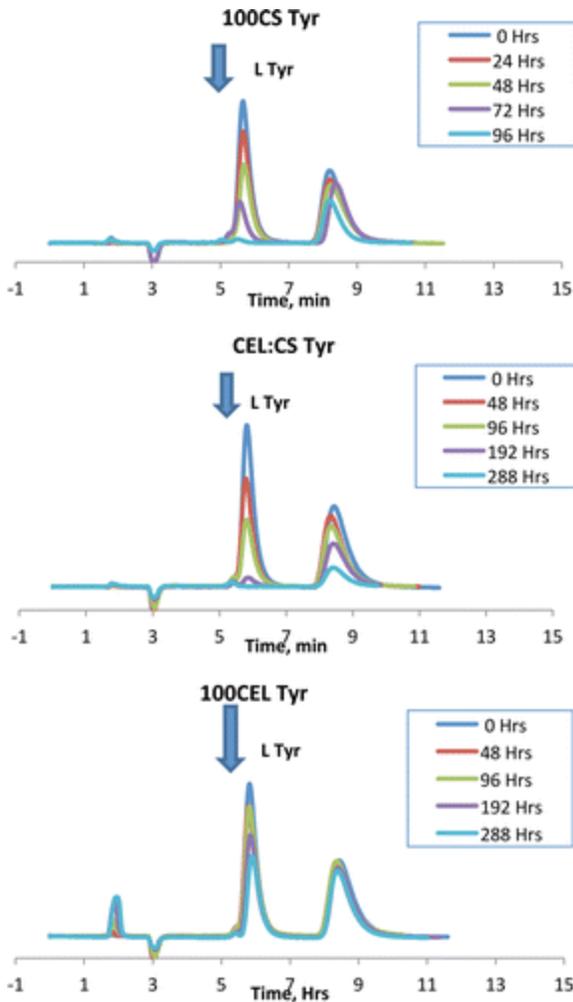
Figure 1. HPLC chromatograms for the sorption of d- and l-Tyr on the different polysaccharide composites.

These HPLC results were then used to calculate the solution concentration of each enantiomer at each measurement time point. The change in solution concentration with time for the three polysaccharide composites is shown in Figure 2A. This figure also illustrates what was observed with the chromatograms where the solution concentrations of the enantiomers are decreasing with time. Also, for each of the three composites, the solution concentration of the l enantiomer (squares, solid line) was found to decrease faster than that of the d enantiomer (diamond, dashed line). From these HPLC results, the amount of each enantiomer that has been adsorbed onto the composite material can be calculated using the following mass balance equation

$$q_t = \left(\frac{C_i - C_t}{m}\right)V$$

(1)

where q_t (mg/g) is the amount of enantiomer adsorbed at any given time, t, C_i and C_t (mg/L) are the initial and time t solution concentrations of the enantiomer, respectively. V (L) is the volume of the solution, and m (g) is the weight of the composite material. Typical results for the adsorption of the d- and l-Tyr forms of a racemic mixture by all three composite materials are shown in Figure 2B. Essentially, these results show similar information that is depicted in Figure 2A; namely, the amount of l enantiomer adsorbed onto the composite material is greater than that of the d enantiomer. For both l and d enantiomers, the order of adsorption capacity

for the composites as explained earlier was found to be 100% CS > [CEL+CS] > 100% CEL. This finding was not unexpected because CS is generally known to be a good adsorbent. The purpose of adding CEL to CS is, as explained before and verified in our previous publication, to improve the poor mechanical and rheological properties of CS.(23-25) The results in Figure 2B show that after about 96 h, 100CS had adsorbed about 5.7 times more l enantiomer than 100% CEL. Interestingly, even though the adsorption of the l enantiomer by the [CEL+CS] composite is expectedly lower than that of 100% CS, it is still about 3.5 times higher than that of the 100% CEL composite material. This adsorption performance is still relatively high considering the improvement in mechanical and rheological properties that is gained by adding 50% CEL to CS. Specifically, as described in our previous publication, whereas the tensile strength of the 50:50 CEL/CS composite material is 2 times greater than that of 100% CS, the swelling in water of the former is only about 1.2 times less than that of the 100CS material.(23-25) These observations clearly indicate that stronger, more stable, effective enantiomeric selective polysaccharide composite materials can be fabricated by judiciously controlling the composition and concentration of the CEL/CS composite.
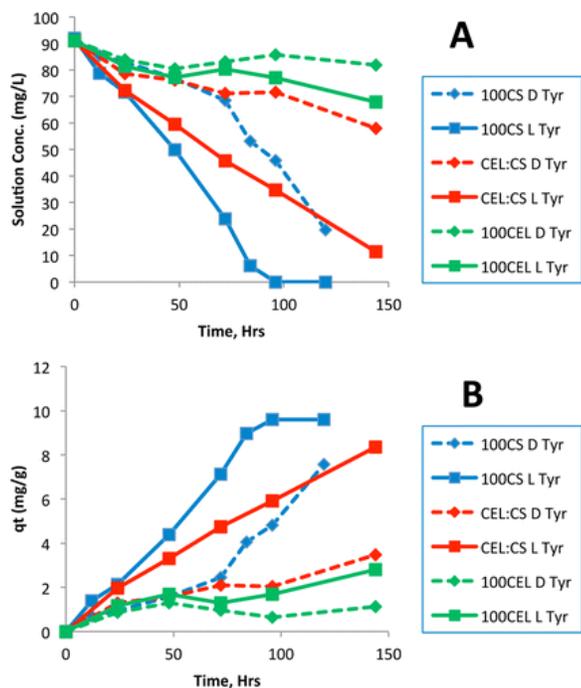

Figure 2. (A) Change in solution concentration with time for a Tyr racemic solution. (B) Adsorption of different Tyr enantiomers by the different composites.

It is possible that for racemic mixtures the presence of one enantiomer may have some effect on the adsorption of other enantiomer. To determine if such an effect is present, the adsorption of optically active (pure) d and l enantiomers was measured separately by UV/vis spectrophometry. The experimental setup and conditions (mass of film and volume of solution) were the same as those used for the racemic mixture. The concentration of the optically active amino acid solutions used for this experiment was 5.0×10^{-4} M, which is the same as that of the individual enantiomers used for the HPLC racemic experiment described above

The results obtained for the adsorption of Tyr enantiomers by all three polysaccharide composite materials, determined by UV/vis, are plotted together with the HPLC results for the racemic experiment (Figure 3). The concentration of each enantiomer in the solution at the beginning of the experiment and the method used for the measurement (HPLC or UV) are indicated in the figure legend. The plots on the left side of the figure are a comparison of the HPLC method and the UV method (Figure 3A–C). It can be seen from this figure that for both methods the adsorption of the l enantiomer is higher than that of the d enantiomer. The results of the UV

method in this figure further confirm that the adsorption of the l enantiomer is selectively favored, even when the enantiomers are measured separately (optically active solutions). However, it can also be observed from this figure that the rate of adsorption of the enantiomers from racemic solutions (HPLC) is different from that of adsorption from optically active solutions (UV). It should be noted, however, that the total amino acid concentration in these two experiments was not the same. The HPLC racemic experiment was performed at a total concentration of 1.0×10^{-3} M (i.e., 5.0×10^{-4} M for each enantiomer). Conversely, the concentration used in the UV experiment for the pure enantiomers was 5.0×10^{-4} M. Because the adsorption capacity is known to be dependent on the type and concentration of chemicals present in the solution, the differences in the type (racemic mixture compared to optically active compounds) and concentration of the amino acid in these two experimental methods may be responsible for the observed differences in the adsorption profiles for the two methods. Nevertheless, additional experiments were then carried out under different conditions to gain more insight into the processes governing the adsorption and ultimately the resolution of the amino acid enantiomers. The results of these experiments are shown in the plots on the right side of Figure 3 (i.e., panels D–F).
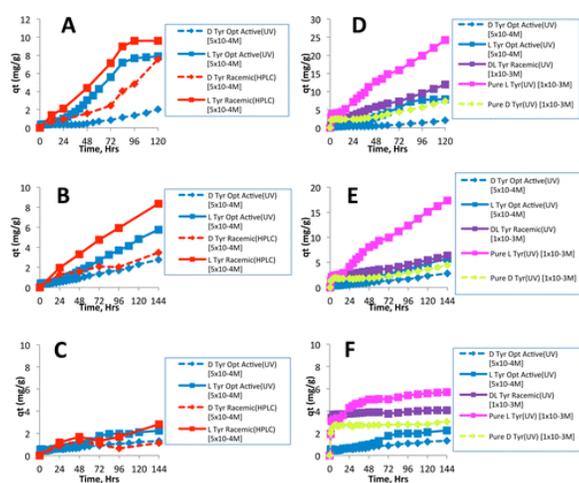

Figure 3. Sorption of d- and l-Tyr enantiomers from different solutions using (A, D) 100% CS, (B, E) the [CEL+CS] composite, and (C, F) the 100CEL composite.

As expected, the adsorption of both d and l enantiomers is dependent not only on the type (ie., optically active or racemic mixture) but also on the concentration of the amino acid present in solution. For example, in the adsorption of d-Tyr (Figure 3D, the right plot), the adsorption profile of d-Tyr in which the initial concentration was 1.0×10^{-3} M (yellow diamond plot) is nearly twice as high as in the sorption profile where the initial concentration was 5.0×10^{-4} M (blue diamond plot). Similarly, the adsorption profile of l-Tyr with an initial concentration of 1.0×10^{-3} M (pink square plot) is also twice as high as the sorption profile where the initial concentration was 5.0×10^{-4} M (blue square plot). However, when the adsorption experiment was done with two samples of the same total concentration but with a different enantiomeric composition (i.e., 1.0×10^{-3} M dl-Tyr racemic mixture (purple square plot) and 1.0×10^{-3} M pure optically active l solution (pink square plot)), interesting adsorption profiles were observed. The adsorption profile of the pure l enantiomer solution was found to be nearly twice as high as that of the dl racemic solution. Because the total amino acid concentration of these two solutions is the same, the observed differences in the adsorption profiles are clearly due to the difference in the enantiomeric composition of the solutions. The solution that gave the highest adsorption profile is that of the pure optically active l solution. The relatively lower adsorptivity observed for the dl racemic mixture can be explained using results previously obtained with HPLC measurements. Specifically, in the HPLC experiments of the racemic mixtures, adsorption favors the l-Tyr component of the dl-Tyr solution, and not much of the d-Tyr component is adsorbed. Because the concentration of the l-Tyr component in this racemic

solution is only half (5.0×10^{-4} M) of that in pure l solution (1.0×10^{-3} M), the adsorption profile of the entire racemic solution equals the adsorption of l-Tyr (i.e., $Q_{l\text{-Tyr}}$) + $Q_{d\text{-Tyr}}$ where $Q_{l\text{-Tyr}}$ is much higher than $Q_{d\text{-Tyr}}$. As a consequence, the adsorption of the racemic mixture is relatively lower than the adsorption of 1.0×10^{-3} M pure optically active l-Tyr. These results are further confirmed by the observation that the adsorption profiles of the 1.0×10^{-3} M dl racemic solution (purple square plot) and the 5.0×10^{-4} M pure l solution (blue square plot) are almost the same. As shown in Figure 3A,D and Figure 3B,E, similar results were observed for both 100% CS and the [CEL+CS] composite, respectively, whereas the trend for the 100CEL material (Figure 3C,F) was not as obvious as a result of the low adsorption capacity of this material.

Additional experiments were also carried out by adsorption of all three composites (100CS, CEL/CS, and 100CEL) of Tyr with the same total concentration but different enantiomeric compositions, namely, a 1.0×10^{-3} M solution that contains 6.67×10^{-4} M l-Tyr and 3.33×10^{-4} M d-Tyr (on HPLC), 1.0×10^{-3} M pure l-Tyr, and 1.0×10^{-3} M dl-Tyr as well as 6.67×10^{-4} M l-Tyr (via UV/vis). The obtained results are plotted together with those previously plotted in Figure 3A–F (for 5.0×10^{-4} M pure l- or pure d-Tyr and 1.0×10^{-3} M dl-Tyr) and shown in Figure SIA–C of the Supporting Information. Again, these results are in agreement with those presented in Figure 3 and further confirm the conclusion described in a previous paragraph; namely, all three 100CS, CEL/CS, and 100CEL composites can enantiomerically adsorb the amino acids, and the adsorption is more favorable to the l enantiomer than to the d enantiomer.

Additional information on the adsorption mechanism can be gained by fitting the experimental data to Weber's intraparticle diffusion model.(26-29) The intraparticle diffusion equation is given as follows(26-29)

$$q_t = k_i t^{1/2} + I$$

(2)

where k_i (mg g^{-1} min$^{-0.5}$) is the intraparticle diffusion rate constant and I (mg g^{-1}) is a constant that gives information regarding the thickness of the boundary layer.(26-29) Shown in Figure 4 are representative intraparticle pore diffusion plots (q_t vs $t^{1/2}$) for different Tyr samples adsorbed on (A) 100% CS, (B) 50:50 CS/CEL, and (C) 100% CEL. It is evident from the figure that there are two separate stages for all Tyr samples on all three composites. In the first linear portion (stage I), the adsorbate molecules (in this case, Tyr molecules) were transported from solution through the solution/composite interface and characterized by k_{i1}. This can be attributed to the immediate utilization of the most readily available adsorbing sites on surfaces of the composites.(26-29) The first stage is followed by a second linear portion in which the adsorbate molecules diffuse into the pores within the particle of the composites and consequently are adsorbed by the interior of each particle, which is measured by k_{i2}.(26-29) Table 1 lists values of k_{i1} and k_{i2} for the adsorption of different Tyr samples by 100% CS, 50:50 CS/CEL, and 100% CEL composite materials. (Similar values for His and Trp are listed in Tables 2 and 3, respectively.) Interestingly, it was found that k_{i2} is much larger than k_{i1} (from 6- to 14-fold) when Tyr molecules are adsorbed by 100% CS. When 50% CEL was added to CS (i.e, the 50:50 CS/CEL composite), k_{i2} is still larger than k_{i1}, but the difference is much smaller than that by the 100% CS composite (0.8- and 7.7-fold compared to 6- and 10-fold). However, in the absence of CS (i.e., the 100% CEL composite), k_{i2} is either smaller than or within experimental error equal to k_{i1}. These results may be explained by the differences in the structure of CS and CEL. It is well known that the strong inter- and intramolecular hydrogen bond network in CEL enables it to adopt a strong and very dense structure that makes it difficult for adsorbate molecules to diffuse from its surface to the interior, thereby leading to relatively low k_{i2} values. Compared to the hydroxy group, the amino group cannot form strong hydrogen bonds. The hydrogen bond network in CS is, therefore, not as extensive as in CEL. As a consequence, the inner structure of CS is relatively less dense than that in CEL. Tyr molecules can, therefore, diffuse from the outer surface to its inner structure relatively more easily than those in CEL. Therefore, k_{i2} values are much larger than k_{i1} and k_{i2} for CEL (because $k_{i2} \approx k_{i1}$ for CEL). It is evident

from Figure 4 and Table 1 that in all Tyr samples and for all three composites k_{i1} is, within experimental error, the same for both enantiomers of l-Tyr whereas k_{i2} for l-Tyr is always higher than that for d-Tyr. The differences are, as expected, largest for 100% CS and smallest for 100% CEL. The results suggest that the enantiomeric selective adsorption is mainly due to the differences not in k_{i1} but rather in k_{i2}. It seems that the binding sites available on the surface of the composites cannot effectively differentiate between l-Tyr and d-Tyr. Enantiomeric selective adsorption is realized as adsorbate molecules diffuse to the interior of the composite because the chirality of CS and CEL makes it possible for them to discriminate chirally against both enantiomers of Tyr, and the discrimination increases as Tyr molecules diffuse into pores of the particle in the interior of the composite. Selectivity is highest for 100% CS because the greater the binding between Tyr molecules to the interior particles, the larger the enantiomeric selectivity.
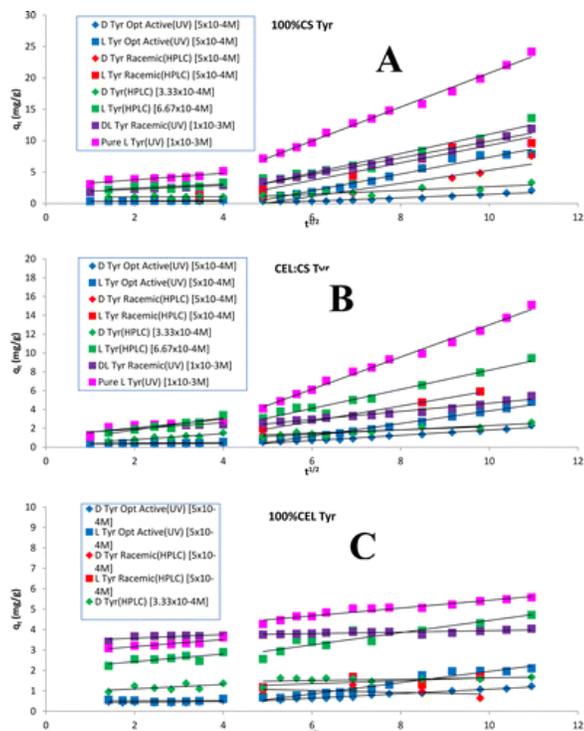

Figure 4. Intraparticle diffusion plots for the sorption of d- and l-Tyr from solutions with different concentrations and/or enantiomeric compositions by (A) 100CS, (B) CEL/CS, and (C) 100CEL composites.

Table 1. Intraparticle Diffusion Model Parameters for the Sorption of Tyr Enantiomers

	100CS				CEL/CS				100CEL			
	k_{i1}	R^2	k_{i2}	R^2	k_{i1}	R^2	k_{i2}	R^2	k_{i1}	R^2	k_{is}	R^2
d-Tyr opt active (UV) (5×10^{-4} M)			0.27 ± 0.02	0.9086			0.28 ± 0.01	0.9769			0.109 ± 0.006	0.9616
l-Tyr opt active (UV) (5×10^{-4} M)			1.34 ± 0.06	0.9722			0.67 ± 0.02	0.9833			0.28 ± 0.02	0.9495
d-Tyr racemic (HPLC) (5×10^{-4} M)			1.0 ± 0.2	0.8455			0.17 ± 0.04	0.8916			− 0.05 ± 0.08	0.1438
l-Tyr racemic (HPLC) (5×10^{-4} M)			1.5 ± 0.1	0.9803			0.81 ± 0.05	0.9933			0.07 ± 0.07	0.3482
d-Tyr (HPLC) (3.33×10^{-4} M)	0.02 ± 0.09	0.0092	0.29 ± 0.06	0.7739	0.27 ± 0.06	0.8518	0.23 ± 0.03	0.8697	0.08 ± 0.08	0.1986	0.03 ± 0.02	0.1974
l-Tyr (HPLC) (6.67×10^{-4} M)	0.2 ± 0.1	0.2970	1.5 ± 0.1	0.9539	0.52 ± 0.09	0.8845	1.02 ± 0.07	0.9658	0.14 ± 0.08	0.4311	0.30 ± 0.04	0.8584
dl-Tyr racemic (UV) (1×10^{-3} M)	0.22 ± 0.02	0.9678	1.34 ± 0.05	0.9841	0.25 ± 0.06	0.8411	0.43 ± 0.02	0.9641	0.12 ± 0.05	0.6042	0.036 ± 0.008	0.6297
pure l-Tyr (UV) (1×10^{-3} M)	0.26 ± 0.04	0.9314	2.71 ± 0.07	0.9935	0.22 ± 0.02	0.9547	1.71 ± 0.04	0.9931	0.13 ± 0.02	0.9580	0.19 ± 0.01	0.9382

The 100% CS has the highest and 100% CEL has the lowest enantiomer selectivity. The fact is that the 50:50 CS/CEL composite exhibits not only relatively high selectivity but also is more similar to 100% CS than to 100% CEL. This is very encouraging because as described in our previous work CS has relatively poor rheological and mechanical properties and is known to undergo swelling in water. Adding CEL to CS not only improves its rheological and mechanical properties but also reduces its swelling.(24, 25) In fact, we showed that adding 50% CEL to CS increases its tensile strength by 2-fold and reduces its swelling by 35%.(24, 25) Taken together, the results indicate that a 50:50 CS/CEL composite has good enantiomer selectivity and adequate rheological properties required for daily practical use.

Table 2. Intraparticle Diffusion Model Parameters for the Sorption of His Enantiomers

	100CS				CEL/CS				100CEL			
	k_{i1}	R^2	k_{i2}	R^2	k_{i1}	R^2	k_{i2}	R^2	k_{i1}	R^2	k_{i2}	R^2
d-His opt active (UV) (5×10^{-4} M)			0.08	0.7954			0.11	0.4983			0.06	0.6409
l-His opt active (UV) (5×10^{-4} M)			1.08	0.9057			0.94	0.9888			0.75	0.7015
d-His racemic (HPLC) (5×10^{-4} M)			0.22	0.9010			0.11	0.8180			0.16	0.9257
l-His racemic (HPLC) (5×10^{-4} M)			1.53	0.9753			1.41	0.9943			1.25	0.9949

The sorption selectivity for the racemic mixtures of different amino acids can be calculated using the following equation(30)

$$\text{sorption seletivity } (\alpha) = \frac{\dfrac{C_{L_i} - C_{L_f}}{C_{L_f}}}{\dfrac{C_{D_i} - C_{D_f}}{C_{D_f}}}$$

(3)

where C_{Li} and C_{Lf} denote the initial and final l concentrations of the l enantiomer and C_{Di} and C_{Df} are the initial and final concentrations of the d enantiomer, respectively. The sorption selectivity was calculated for the HPLC experiments with 1.0×10^{-3} M racemic solutions after 96 h. The 96 h time period was selected because this was generally the amount of time it took for the HPLC band of the l enantiomer to disappear for the 100CS composite material. Results obtained for different amino acids together with the amount of each enantiomer adsorbed at this time are shown in Figure 5. The sorption selectivity is indicated by the gray bars, and adsorbed l and d enantiomers are shown as green diamonds and red squares, respectively. It is clear that except for Phe, for the other three amino acids (Tyr, Trp, and His), the enantioselectivity of the different composites was found to follow the order 100CS > CEL/CS > 100CEL. Because the amount of amino acid adsorption is highest for 100CS and lowest for 100CEL with that for CEL/CS in the middle, the order of enantioselectivity seems to be closely related to the adsorbed amount of amino acid. Also, the amount of l enantiomer adsorbed is progressively larger than that of the d enantiomer, and again the largest difference was found to be the largest for 100CS and smallest for 100CEL. As explained in a previous section, this was the reason for the 100CS composite to have the highest sorption selectivity. Interestingly, different from the other three amino acids, Phe exhibits different selectivity for all three composites. The adsorbed amounts of d-Phe and l-Phe were generally the same for 100% CS, 50:50 CS/CEL, and 100% CEL. Furthermore, the amount of l-Phe adsorbed by the 100CS composite was unexpectedly lower compared to that of the other three amino acids. This might have contributed to the relatively low selectivity observed for Phe with this composite material. Also, it is possible that the enantioselectivity is also dependent on the initial amino acid concentration. Further study is needed to determine this possibility.

Table 3. Intraparticle Diffusion Model Parameters for the Sorption of Trp Enantiomers

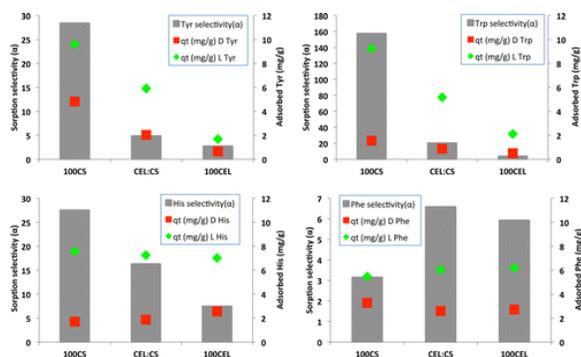|	100CS				CEL/CS				100CEL			
	k_{i1}	R^2	k_{i2}	R^2	k_{i1}	R^2	k_{i2}	R^2	k_{i1}	R^2	k_{i2}	R^2
d-Trp opt active (UV) (5×10^{-4} M)			0.21	0.9038			0.18	0.9525			0.04	0.8653
l-Trp opt active (UV) (5×10^{-4} M)			0.71	0.9712			0.55	0.9832			0.25	0.9905
d-Trp racemic (HPLC) (5×10^{-4} M)			0.21	0.3962			0.10	0.5193			0.06	0.0782
l-Trp racemic (HPLC) (5×10^{-4} M)			1.44	0.9224			0.84	0.9924			0.36	0.8891

Figure 5. Comparison of the selectivity of the different composite materials with the four amino acids studied. The initial concentration of each racemic amino acid was 1.0×10^{-3} M.

Conclusions

The polysaccharide composite materials developed here have shown promising potential applications in chiral separations. Preliminary results with four different amino acids show that racemic mixtures can potentially be resolved by selective adsorption of the l enantiomer in a period from about 96 to 120 h for the 100% CS composite material. The [CEL+CS] composite material, which has relatively superior rheological and mechanical properties, also exhibits good enantioselectivity. The analysis of the enantiomeric adsorption using the intraparticle diffusion model showed that very little to no adsorption was occurring in the first 16 h. This is then followed by a period of steady adsorption in which the intraparticle diffusion rate constant of the l enantiomer is higher than that of the d enantiomer. This difference in diffusion rate constants possibly plays a significant role in the enantiomeric resolution that was observed with these polysaccharide composite materials.

Supporting Information

Plots of adsorption of Tyr solutions with different concentrations and/or enantiomeric compositions by 100CS, CEL/CS, and 100CEL as determined by both UV/vis and chiral HPLC. This material is available free of charge via the Internet at http://pubs.acs.org.

Terms & Conditions

Acknowledgment

References

1 Chem. Eng. News **1990**, 68, 38–– 44. Chem. Eng. News **1992**, 70, 46– 79. Chem. Eng. News **2001**, 79, 45– 56 and 79– 97.

2 Armstrong, D. W.; Han, S. H. Enantiomeric separations in chromatography CRC Crit. Rev. Anal. Chem. **1988**, 19, 175

3 Hinze, W. H. Applications of cyclodextrins in chromatographic separations and purification methods Sep. Pur. Methods **1981**, 10, 159

4 Armstrong, D. W. Optical isomer separation by liquid chromatography Anal. Chem. **1987**, 59, 84A

5 Hinze, W. L.; Armstrong, D. W. Organized surfactant assemblies in separation science ACS Symp. Ser. **1987**, 342, 2– 82

6 Tran, C. D.; Kang, J. Chiral separation of amino acids by capillary electrophoresis with octyl-β-thioglucopyranoside as chiral selector J. Chromatogr., A **2002**, 978, 221– 230

7 Tran, C. D.; Kang, J. Chiral separation of amino acids by capillary electrophoresis with 3-[(3-cholamidopropyl)-dimethylammonio]-1-propane sulfonate (CHAPS) as chiral selector Chromatographia **2003**, 57, 81– 86

8 Zhou, Z.; Xiao, Y.; Hatton, T. A.; Chung, T.-S. Effects of spacer arm length and benzoation on enantioseparation of performance of beta-cyclodextrin fuctionalized cellulose membrances J. Membr. Sci. **2009**, 339, 21– 27

9 Xiao, Y. C.; Chung, T. S. Functionalization of cellulose dialysis membranes for chiral separation using β-cyclodextrin immobilization J. Membr. Sci. **2007**, 290, 78– 85

10 Zhou, Z.; Cheng, J.-H.; Chung, T.-S.; Hatton, T. A. The exploration of the reversed enantioselectivity of a chitosan functionalized cellulose acetate membranes in an electric field driven process J. Membr. Sci. **2012**, 389, 372– 379

11 Finkenstadt, V. L.; Millane, R. P. Crystal structure of *Valonia* cellulose 1β Macromolecules **1998**, 31, 7776– 7783

12 Augustine, A. V.; Hudson, S. M.; Cuculo, J. A. Cellulose Sources and Exploitation. In Kennedy, J. F.; Philipps, G. O.; Williams, P. A., Eds.; New York: E. Horwood: 1990, p 59.

13 Kadokawa, J.; Murakami, M.; Kaneko, Y. A facile method for preparation of composites composed of cellulose and a polystyrene-type polymeric ionic liquid using a polymerizable ionic liquid Compos. Sci. Technol. **2008**, 68, 493– 498

14 Dawsey, T. R. Cellulosic Polymers, Blends and Composites; Carl Hanser Verlag: New York, 1994.

15 Dai, T.; Tegos, G. P.; Burkatovskaya, M.; Castano, A. P.; Hamblin, M. R. Chitosan acetate bandage as a topical antimicrobial dressing for infected burns Antimicrob. Agents Chemother. **2009**, 53, 393– 400

16 Bordenave, N.; Grelier, S.; Coma, V. Hydrophobization and antimicrobial activity of chitosan and paper-based packaging material Biomacromolecules **2010**, 11, 88– 96

17 Rabea, E. I.; Badawy, M. E. T.; Stevens, C. V.; Smagghe, G.; Steurbaut, W. Chitosan as antimicrobial agent: applications and mode of action Biomacromolecules **2003**, 4, 1457– 1465

18 Burkatovskaya, M.; Tegos, G. P.; Swietlik, E.; Demidova, T. N.; Castano, A. P.; Hamblin, M. R. Use of chitosan bandage to prevent fatal infections developing from highly contaminated wounds in mice Biomaterials **2006**, 27, 4157– 4164

19 Kiyozumi, T.; Kanatani, Y.; Ishihara, M.; Saitoh, D.; Shimizu, J.; Yura, H. Medium (DMEM/F12)-containing chitosan hydrogel as adhesive and dressing in autologous skin grafts and accelerator in the healing process J. Biomed. Mater. Res. B: Appl. Biomater. **2006**, 79B, 129– 136

20 Jain, D.; Banerjee, R. Comparison of ciprofloxacin hydrochloride-loaded protein, lipid, and chitosan nanoparticles for drug delivery J. Biomed. Mater. Res. B: Appl. Biomater. **2008**, 86, 105– 112

21 Tirgar, A.; Golbabaei, F.; Hamedi, J.; Nourijelyani, K.; Shahtaheri, S.; Moosavi, S. Removal of airborne hexavalent chromium mist using chitosan gel beads as a new control approach Int. J. Environ. Sci. Technol. **2006**, 3, 305– 313

22 Nishiki, M.; Tojima, T.; Nishi, N.; Sakairi, N. β-Cyclodextrin-linked chitosan beads: preparation and application to removal of bisphenol A from water Carbohydr. Lett. **2000**, 4, 61– 67

23 Duri, S.; Tran, C. D. Supramolecular composite materials from cellulose, chitosan, and cyclodextrin: facile preparation and their selective inclusion complex formation with endocrine disruptor Langmuir **2013**, 29, 5037– 5049

24 Tran, C. D.; Duri, S.; Harkins, A. L. Recyclable synthesis, characterization and antimicrobial activity of cellulose-based polysacchrdie composite materials J. Biomed. Mater. Res. A **2013**, 1– 10

25 Tran, C. D.; Duri, S.; Delneri, A.; Franko, M. Chitosan-cellulose composite materials: preparation, characterization and application for removal of microcystin J. Hazard. Mater. **2013**, 252–253, 355– 366

26 Weber, J. W.; Morris, J. C. Kinetics of adsorption of carbon from solution J. Sanit. Eng. Div. Am. Soc. Civ. Eng. **1963**, 89, 31– 39

27 Hameed, B. H.; Chin, L. H.; Rengaraj, S. Adsorption of 4-chlorophenol onto activated carbon prepared from rattan sawdust Desalination **2008**, 225, 185– 198

28 Elsherbiny, A. B.; Salem, M. A.; Ismail, A. A. Influence of alkyl chain length of cyanine dyes on adsorption by Na^+-montmorillonite from aqueous solutions Chem. Eng. J. **2012**, 200, 283– 290

29 Gu, W.; Sun, C.; Liu, Q.; Cui, H. Adsorption of avermectins on activated carbon: equilibrium, kinetics, and UV-shielding Trans. Nonferrous Met. Soc. China **2009**, 19, 845– 850

30 Wang, H.-D.; Chu, L.-Y.; Song, H.; Yan, J.-P.; Xie, R.; Yang, M. Preparation and enantiomer separation characteristics of chitosan/β-cyclodextrin composite membranes J. Membr. Sci. **2007**, 297, 262– 270